

# Optically switching the THz transmission of metallic sub-wavelength hole arrays

E. Hendry<sup>1,2\*</sup>, M.J. Lockyear<sup>1</sup>, J. Gómez Rivas<sup>2</sup>, L. Kuipers<sup>2</sup> and M. Bonn<sup>2</sup>

<sup>1</sup> *School of Physics, University of Exeter, Stocker Road, Exeter, EX4 4QL, UK.*

*Fax: +44 1392 264104*

*E-mail: e.hendry@exeter.ac.uk*

<sup>2</sup> *FOM Institute for Atomic and Molecular Physics, Kruislaan 407, 1098 SJ, Amsterdam, The Netherlands*

We demonstrate optical switching of the enhanced transmission of TeraHertz radiation through a metal grating with sub-wavelength holes. By fabricating the grating on a semiconductor silicon substrate, we are able to control the grating transmission intensity by varying the photo-doping level of the silicon, switching the transmission on picosecond timescales with low visible light intensities.

PACS numbers: 73.20.Mf, 41.20.Jb, 42.25.Fx, 78.47.+p

Thin metal films with a two-dimensional periodic array of sub-wavelength holes can exhibit anomalously high transmission at certain wavelengths above the cut-off for the aperture [1]. It is thought that the mechanism behind this enhanced transmission involves coupling to surface plasmon polaritons (SPPs). Nevertheless, the highly frequency-dependent transmission, as well as the high localized electric field strengths at the metal interface, mean that such metal film gratings are finding applications in visible spectroscopy [2], sub-wavelength optics [3], non-linear optics [4], and photolithography [5].

More recently, enhanced transmission through metal [6-8] and semiconductor [9-11] arrays has been observed in the THz frequency regime, and there are some reports of an even larger enhancement than at optical frequencies [12]. While enhanced transmission through such sub-wavelength arrays is understandably of technological interest, the ability to control and switch the transmission would be of considerable significance, in particular for high bandwidth and/or time resolved applications. Rivas et al. [13] have recently demonstrated thermal switching of the THz transmission by modifying the density of free carriers in a silicon grating with temperature, while Pan et al. [14] demonstrated magnetic switching, by using a nematic liquid crystal as medium filling the of a metal grating. Optical control has also recently been demonstrated for semiconductor hole arrays [15], where photoexcitation of a semiconductor hole array using a powerful continuous wave laser source allowed tuning of surface photo-electron/hole densities and coupling to SPPs. All of these control techniques are, however, inherently slow processes, making these approaches inapplicable when fast switching is required.

In this contribution we present measurements of enhanced THz transmission through periodic arrays of sub-wavelength holes in thin gold films on silicon. Sharp resonances are observed in the transmission spectrum at wavelengths related to the lattice dimensions. By fabricating the metal array on a semiconductor substrate we are able to finely control the transmission intensities of the grating through above band-gap photo-excitation of the semiconductor substrate. It is shown that the transmission can be switched on picosecond timescales with relatively low intensities of visible light.

The samples are fabricated by contact lithography on a 1 mm thick wafer of silicon to define the structure on a photo-resist, followed by the evaporation of a film of 200 nm of gold and a lift-off process to generate the array of holes. Fig. 1(a) shows an optical microscope image of our sample: it consists of a gold layer with square holes (length  $a=38 \mu\text{m}$  with lattice spacing  $L=100 \mu\text{m}$ ). While a homogeneous gold layer of 200 nm is completely opaque to THz radiation, the silicon wafer substrate exhibits close to 100 % transmission.

We measure the zero order transmission of the grating using a THz spectrometer similar to that described in Ref. [16]. The incident THz pulses are essentially single cycle electromagnetic pulses of about 1ps duration and peak field strength  $\sim 1 \text{ kV/cm}$  when focused for detection. The time-dependent field strengths at normal incidence are detected directly in the far field, with and without sample ( $E(t)$  and  $E_0(t)$ , respectively) – see inset of fig. 1(b), measured using a collimated beam with a beam diameter  $\sim 10 \text{ mm}$ . By Fourier transforming the time waveforms the intensity transmission spectrum,  $I(\omega)=|E(\omega)|^2/|E_0(\omega)|^2$ , is calculated – plotted in figure 1(b) as a function of wavelength  $\lambda$ . The spectral resolution

of fig. 1(b) is 66 GHz (or 18  $\mu\text{m}$  at 300  $\mu\text{m}$ ), corresponding to a time window of 15 ps, dictated by multiple reflections within the silicon wafer. The spectrometer is flushed with dry nitrogen gas in order to prevent absorption by water vapor.

We observe clear resonances in fig. 1(b) at  $\lambda \sim 100 \mu\text{m}$ , 150  $\mu\text{m}$ , 170  $\mu\text{m}$ , 250  $\mu\text{m}$  and 350  $\mu\text{m}$ , and measure a very similar spectrum if the sample is reversed and the THz pulses propagate through the silicon first. The prevailing explanation for the enhanced transmission of periodic hole arrays involves coupling SPPs on both interfaces of the array [3]. The wavelengths of SPPs on a grating interface under normal incidence are approximately given by [3]

$$\lambda = \frac{l}{\sqrt{i^2 + j^2}} \times \sqrt{\frac{\epsilon_d \epsilon_m}{\epsilon_d + \epsilon_m}}, \quad (1)$$

dependent on  $i$  and  $j$ , the integer mode indices, and on the dielectric functions of the dielectric ( $\epsilon_d$ ) and metal ( $\epsilon_m$ ) at the interfaces. For our gratings, eq. (1) has two sets of solutions: for the air-gold interface ( $\epsilon_d = \epsilon_{\text{air}}$ ,  $\epsilon_m = \epsilon_{\text{gold}}$ ) and for the gold-silicon interface ( $\epsilon_m = \epsilon_{\text{gold}}$ ,  $\epsilon_d = \epsilon_{\text{Si}}$ ). In the THz frequency regime,  $\epsilon_{\text{gold}} \gg \epsilon_{\text{air}} = 1$  and  $\epsilon_{\text{Si}} = 11.9$ . The arrows in fig. 1(b) (in order of increasing wavelength) represent the ( $i=1, j=0$ ) mode for the air-gold interface, and the (2,1), (2,0), (1,1) and (1,0) modes for the gold-silicon interface. All of the transmission resonances in fig. 1(b) are at wavelengths significantly larger than the cut off wavelength  $\sim 76 \mu\text{m}$  for square holes with  $a=38 \mu\text{m}$  [17], so the transmission of a *single* hole should be very small. Despite this, the (1,1) and (1,0) modes for the silicon interface especially give rise to large, well defined peaks in our transmission spectrum at 250  $\mu\text{m}$

and 350  $\mu\text{m}$  respectively, similar to previously reports of THz transmission through metal hole arrays [7, 8, 18].

We can optically modify the THz dielectric function of the silicon with above band-gap photoexcitation (indirect gap $\sim$ 1.1 eV, direct gap $\sim$ 3.2 eV [19]). This photoexcitation is achieved using either 1.5 eV or 3.1 eV photons in 150 fs laser pulses. To allow spatial overlap of the THz light with the excitation pulses we weakly focus the THz pulses onto the sample using parabolic mirrors (focal length 6 cm, numerical aperture of 0.18) resulting in a beam waist of 1.8 mm in diameter, allowing illumination of  $\sim$ 300 holes. In this configuration, the transmission peaks are significantly broadened as a result of the distribution of incident wave vectors. Details of this effect will be presented in a later contribution.

In fig.2 (a) and (b) we compare transmission spectra after excitation of the back and front interfaces of the sample respectively, as defined in the inset of fig. 2(c), measuring 10 ps after photo-excitation with 3.1 eV photons. It should be noted that, since we are close to the direct band gap of silicon with 3.1 eV photons, the penetration depth of the light ( $\sim$ 125 nm [19]) is significantly smaller than the thickness of the silicon (1 mm). Photo-excitation then introduces a very thin, partially conducting layer essentially at the surface of the silicon. By photo-excitation of the *back* interface we can control the transmission simply by regulating the absorption of this photo-active layer. As can be seen from the absence of any peak shifting in fig. 2(a), photoexcitation of the back interface does not alter the spectral profile of transmission, and requires substantial intensities for a significant drop in transmission.

By photo-exciting the *front* side (fig. 2(b)) we create conducting regions in the silicon regions near the holes in the gold layer. One might expect that this could allow the SPP at the silicon-gold interface to bridge the hole without scattering, thereby reducing the coupling to diffracted modes on the silicon side of the grating. Indeed, photoexcitation of the front interface of the grating very strongly decreases the transmission: for a relatively weak fluence of  $0.1 \text{ J/m}^2$ , excitation of the back interface reduces transmission by 20 %, while excitation of the front interface reduces transmission by almost a factor of 5. This difference is highlighted in fig. 2(c), where the dots indicate the transmission after photo-exciting the front and back interfaces with identical intensities. The linear solid line in fig. 2(c) shows the trend expected for purely absorption. The trend in the data points is significantly stronger than this: the dotted line represents a cubic dependence. This suggests that the effect described above, in addition to absorption, may reduce the transmission when photo-exciting the front interface. Furthermore, transmission after photo-excitation of the front interface is also strongly dependent on the energy of excitation photons: the transmission after *front* excitation by 1.5 eV photons ( $0.1 \text{ J/m}^2$ ) is compared in fig. 2(d). With 1.5 eV photons we excite well below the direct band gap of silicon, resulting in a significantly larger the penetration depth of the light ( $\sim 1 \text{ }\mu\text{m}$  at 300 K [19]), reducing the electron density at the gold interface and increasing transmission through the grating.

In order to confirm the explanation outlined above, we have carried out finite element method modeling (FEM) of the system, approximating the photo-excited region as a 125 nm homogenous layer below the holes. The intensity dependent dielectric function of this region is calculated with the Drude model according to ref. [20]. Fig. 3(a) shows the

electric field magnitude for  $\lambda=346 \mu\text{m}$  (corresponding to the (1,0) resonant transmission for the silicon-gold interface) with and without  $0.1 \text{ J/m}^2$ ,  $3.1 \text{ eV}$  excitation. The modeling clearly shows that photoexcitation of the silicon reduces the electric field in the diffracted orders on the silicon side of the grating. Fig. 3(b) shows the change in diffracted intensity is predominantly caused by an increase in *reflection* from the grating. The change in absorbance is significantly smaller, accounting for  $< 10\%$  of the observed change in the peak transmission.

Though the wavelength of resonant transmission agrees well with experiment, the magnitude and width of transmission peaks are significantly larger and smaller respectively in the modeled data. This is due to a combination of several effects, including beam convergence, spectral resolution and sample inhomogeneity. The model does predict the red slight shift in transmission maxima observed in experiment (around  $20 \mu\text{m}$  – see vertical dotted lines in fig. 2(a)), as well as the broadening of transmission peaks on photoexcitation, though these effects are again smaller in the modeled data.

While the modification of the transmission spectral profile is beneficial for many applications, one of the main advantage that optical switching of transmission offers over thermal [13] and magnetic [14] switching is fast switching times. In fig. 4(a) we plot the transmission spectrum as a function of time after excitation with  $1 \text{ J/m}^2$ ,  $1.5 \text{ eV}$  photon pulses, measured and calculated according to refs. [16, 21]: within one picosecond transmission is reduced to  $< 3 \%$  over the entire probe spectral range. The blue dotted line in fig. 4(b) represents a vertical cut of the data in fig. 4(a) for  $\lambda=250 \mu\text{m}$ : the decay is approximately exponential, with a time constant of approximately  $280 \text{ fs}$ . Also plotted are

the transmission dynamics of a pure silicon wafer under the same excitation conditions (solid black line), scaled to match the array data. The similarity between two traces suggests that transmission dynamics of the hole array are determined by the bulk cooling of photoelectrons in silicon. We also observe that excitation with higher energy photons ( $\sim 1 \text{ J/m}^2$ , 3.1 eV photon pulses) leads to slower dynamics (red dashed line), consistent with previous THz measurements of carrier cooling in bulk semiconductors [22]. Therefore, by using photon energies exactly matched to the band gap of the material it should be possible to reduce transmission on even faster timescales, essentially determined by the temporal width of the excitation pulse. It should be noted, however, that switching times for any optical switch are restricted by the *recovery* time of transmission. Since silicon is an indirect band gap semiconductor, photoconductivity decay (and transmission recovery) will involve trapping and eventual recombination at impurity centers. At low temperature and low carrier densities this can be a fairly efficient process [23], and at 20 K and  $0.1 \text{ J/m}^2$  excitation we observe a sub-nanosecond recovery of transmission (see inset of fig. 4(b)). At room temperature, recovery times are significantly longer, extending to microseconds. Shorter recovery times at room temperature may be achieved by using a direct band-gap semiconductor. It should be noted that these switching times are significantly faster than the ( $>$  millisecond) switching times attainable for the thermal [13] and magnetic [14] switching described in the introduction.

To conclude, we have demonstrated optical switching and some degree of tunability in the transmission of a sub-wavelength metal hole array in the THz frequency range. By fabricating the grating on a semiconductor substrate, visible light can be used to modify the

electron density in the semiconductor, and thereby control the THz transmission of the grating. The fast switching in transmission has implications for time-resolved and high bandwidth applications. Moreover, by photo-exciting with photon energies close to the direct band gap of silicon (3.2 eV [19]) transmission can be controlled with very low light intensities.

This work is part of the research program of the "Stichting voor Fundamenteel Onderzoek der Materie (FOM)", which is financially supported by the "Nederlandse organisatie voor Wetenschappelijk Onderzoek (NWO)". The authors would like to thank F.J. Garcia-Vidal and J.R. Sambles for helpful discussions.

## References

- [1] T. W. Ebbesen, et al., *Nature* **391**, 667 (1998).
- [2] J. V. Coe, et al., *Anal. Chem.* **78**, 1384 (2006).
- [3] W. L. Barnes, A. Dereux, and T. W. Ebbesen, *Nature* **424** (2003).
- [4] J. A. H. v. Nieuwstadt, et al., *Phys. Rev. Lett.* **97**, 146102 (2006).
- [5] X. G. Luo and T. Ishihara, *Opt. Express* **12**, 3055 (2004).
- [6] D. Qu, D. Grischkowsky, and W. Zhang, *Opt. Lett.* **29**, 896 (2004).
- [7] F. Miyamaru and M. Hangyo, *Appl. Phys. Lett.* **84**, 2742 (2004).
- [8] J. O'Hara, R. D. Averitt, and A. J. Taylor, *Opt. Express* **12**, 6397 (2004).
- [9] J. G. Rivas, C. Schotsch, P. H. Bolivar, and H. Kurz, *Phys. Rev. B* **68**, 201306 (2003).
- [10] C. Janke, et al., *Phys. Rev. B* **69**, 205314 (2004).
- [11] A. K. Azad, Y. Zhao, and W. Zhang, *Appl. Phys. Lett.* **86**, 141102 (2005).
- [12] H. Cao and A. Nahata, *Opt. Express* **12**, 1004 (2004).
- [13] J. G. Rivas, P. H. Bolivar, and H. Kurz., *Opt. Lett.* **29**, 1680 (2004).
- [14] C. L. Pan, et al., *Opt. Express* **13**, 3921 (2005).
- [15] J. G. R. C. Janke, P. Haring Bolivar, H. Kurz, *Opt. Lett.* **30**, 2357 (2005).
- [16] E. Hendry, et al., *Phys. Rev. B* **71**, 125201 (2001).
- [17] J. B. Pendry, L. Martin-Moreno, and F. J. Garcia-Vidal, *Science* **305**, 847 (2004).
- [18] D. Qu, D. Grischkowsky, and W. Zhang, *Opt. Lett.* **29**, 896 (2004).
- [19] G. E. Jellison and F. A. Modine, *Appl. Phys. Lett.* **41**, 180 (1982).

- [20] E. Hendry, M. Koeberg, J. Pijpers and M. Bonn, "Reduction of carrier mobility in semiconductors caused by charge-charge interactions."
- [21] J. T. Kindt and C. A. Schmuttenmaer, *J. Chem. Phys.* **110**, 8589 (1999).
- [22] P. N. Saeta, et al., *Appl. Phys. Lett.* **60**, 1477 (1992).
- [23] A. Hangleiter, *Phys. Rev. B* **35**, 9149 (1987).

## Figures

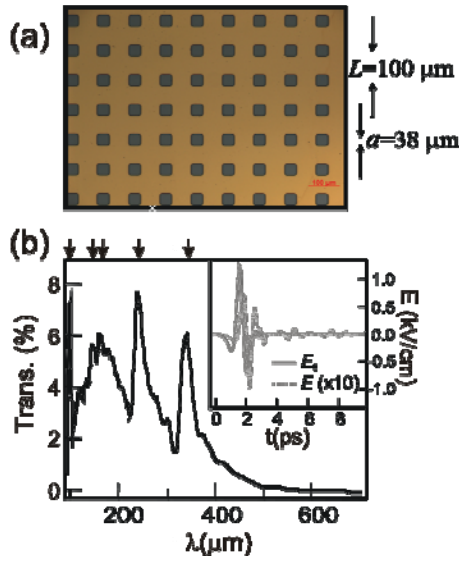


FIG. 1. (a) Optical microscope image of the sample, showing gold (brown) and silicon (black) regions. (b) The transmission spectrum for plane wave transmission. The arrows indicate peak wavelengths predicted by eq. (1). Inset: The time domain measurements of the transmitted and reference electric fields.

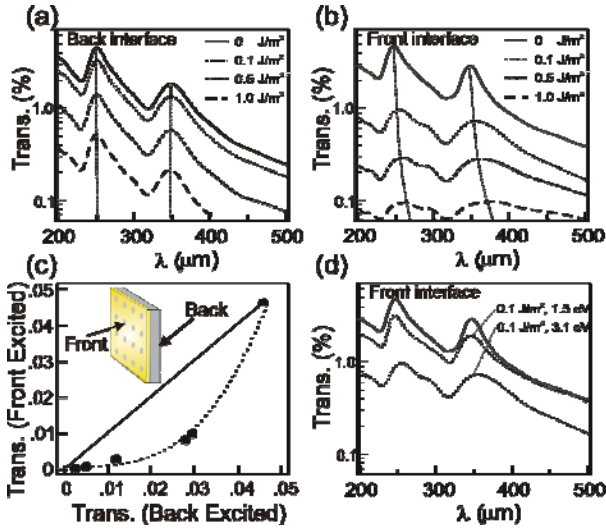


FIG. 2 (a) Normalized transmission spectra measured 10 ps after photo-excitation of the *front* interface of the grating using 3.1 eV photon pulses. (b) Normalized spectra after excitation of the *back* interface. (c) Dots indicate the transmission after photo-exciting the front and back interfaces with identical intensities. The linear solid line is the trend expected if the photoexcited silicon is purely absorbing THz radiation, while the dotted line represents a cubic dependence. (d) Comparison between excitation of the front interface with 1.5 eV photons and 3.1 eV photons.

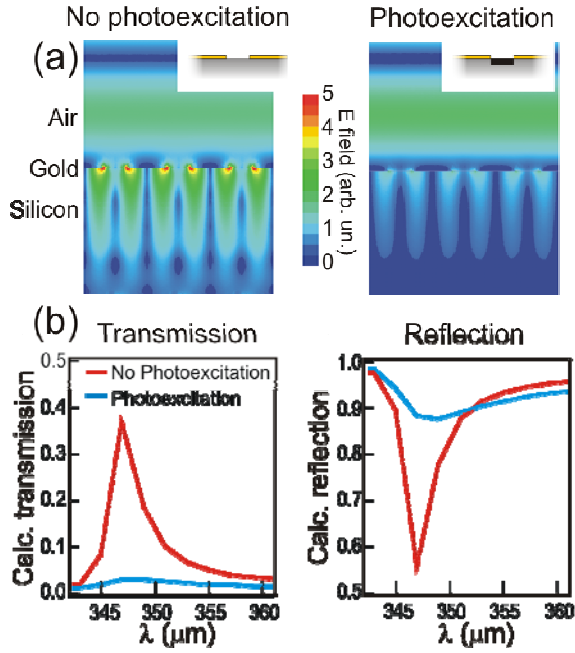


FIG. 3. (a) FEM showing the electric field strength in the diffracted orders with and without photo-excitation by  $0.1 \text{ J/m}^2$ ,  $3.1 \text{ eV}$  pulses. The excitation region is treated as a homogenous layer below the holes,  $125 \text{ nm}$  deep (black region in inset). (b) The change in diffracted intensity on photo-excitation is predominantly caused by an increase in *reflection* from the grating.

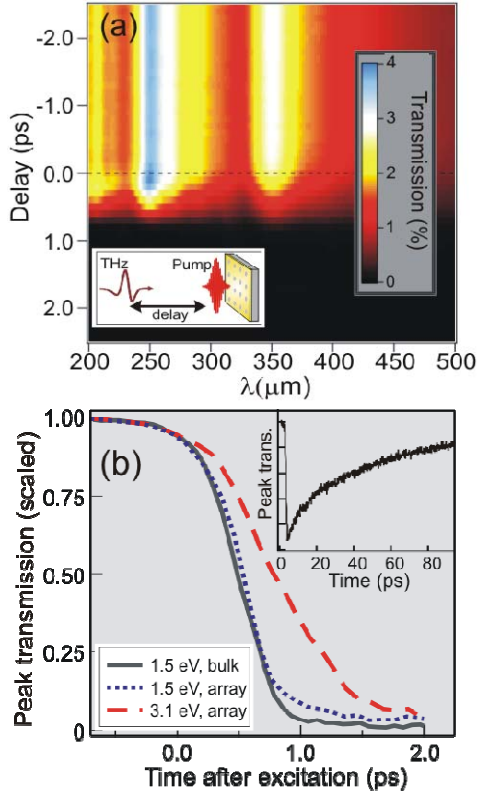


FIG. 4. (a) Transmission spectrum measured as a function of time after excitation using  $1 \text{ J/m}^2$ , 1.5 eV photon pulses. (b) Comparison of switching dynamics: peak transmission (at  $250 \text{ }\mu\text{m}$ ) as a function of time for bulk silicon (black solid line) and hole array (blue dotted line) after excitation by 1.5 eV photons, and hole array (red dashed line) after excitation by 3.1 eV photons. Inset: recovery time for  $0.1 \text{ J/m}^2$  at 20 K.